Preparation of Nanoporous Polyelectrolyte Multilayer Films via Nanoparticle Templating

Qi Li, John F. Quinn, Yajun Wang, and Frank Caruso*

Centre for Nanoscience and Nanotechnology, Department of Chemical and Biomolecular Engineering, The University of Melbourne, Victoria 3010, Australia

Received July 13, 2006. Revised Manuscript Received August 24, 2006

Polyelectrolyte−nanoparticle hybrid multilayer films were used as templates for the preparation of nanoporous polymer thin films. The hybrid multilayers were constructed by consecutively depositing an anionic blend of silica nanoparticles (SiO_2 NPs) and poly(acrylic acid) (PAA) and a cationic polyelectrolyte, poly(allyamine hydrochloride) (PAH). Layer-by-layer growth of the multilayers with different SiO_2 NP sizes (25, 45, and 85 nm in diameter) and at different pH was followed by quartz crystal microgravimetry (QCM). Film buildup, as assessed by QCM mass changes, was 3 times larger when assembled with PAH at pH 9 than with PAH at pH 5. After chemically cross-linking the PAA/PAH within the films, the SiO_2 NPs were removed by dissolution with hydrofluoric acid. Atomic force microscopy and transmission electron microscopy were used to characterize the porous films formed and revealed that the pore size could be controlled by using SiO_2 NPs of different size. The adsorption of bovine serum albumin (BSA) on the porous thin films showed that the amount of BSA adsorbed increased with increasing bilayer number, suggesting the protein infiltrated the films. This provides opportunities to tune the protein content in the films, which is of interest for applications in biocatalysis and biosensing.

Introduction

Polymer materials containing nanopores have diverse applications in separations,[1,2] catalysis,[3,4] antireflection coatings,[5] sensing,[6,7] biomaterials engineering,[6] and templates for fabricating various nanoscopic materials.[8,9] This has motivated the development of various methods for preparing nanoporous polymer materials with tunable pore sizes. For instance, phase separation of block copolymers has been exploited to prepare polymer materials with well-defined, ordered arrays of nanostructured domains.[10,11] Further, replicating mesoporous silica templates or sacrificial colloidal crystal templates by polymerization or polymer casting within the interstitial voids, followed by template removal, results in porous polymers.[6,12−16] Other methods for preparing porous polymer materials include selective degradation of block copolymer domains, selective dissolution of polymer blends, surfactant templating, and CO_2 foaming.[5,17−20]

Methods for introducing porosity in layer-by-layer (LbL) polyelectrolyte multilayer (PEM) thin films have also been reported in recent years. Rubner and co-workers prepared porous thin films by inducing polymer rearrangement in weak PEMs of poly(acrylic acid)/poly(allylamine hydrochloride) (PAA/PAH) by exposing the films, post-assembly, to a low pH solution.[21,22] We showed that porous PAA/PAH films were also obtained by exposing the PEMs prepared from salt-containing polyelectrolyte solutions to pure water.[23]

Over the past decade, the LbL technique has been developed into an important and versatile method for the fabrication of thin films with tailorable thickness and properties. In addition to the typical alternate deposition between two solutions containing a single component, recent studies have demonstrated that by having two components in one of the adsorption solutions, film properties such as thickness, composition, and pH response can be easily

* Corresponding author. Fax: +61 3 8344 4153. E-mail: fcaruso@unimelb.edu.au.

(1) Hilder, E. F.; Svec, F.; Frechet, J. M. J. *Anal. Chem.* **2004**, *76*, 3887.
(2) Lakshmi, B. B.; Martin, C. R. *Nature* **1997**, *388*, 758.
(3) Sharma, A. C.; Borovik, A. S. *J. Am. Chem. Soc.* **2000**, *122*, 8946.
(4) Sedlacek, J.; Pacovska, M.; Redrova, D.; Balcar, H.; Biffis, A.; Corain, B.; Vohlidal, J. *Chem. Eur. J.* **2002**, *8*, 366.
(5) Walheim, S.; Schaffer, E.; Mlynek, J.; Steiner, U. *Science* **1999**, *283*, 520.
(6) Li, Y. Y.; Cunin, F.; Link, J. R.; Gao, T.; Betts, R. E.; Reiver, S. H.; Chin, V.; Bhatia, S. N.; Sailor, M. J. *Science* **2003**, *299*, 2045.
(7) Sugimoto, I. *Analyst* **1998**, *123*, 1849.
(8) Jiang, P.; Bertone, J. F.; Colvin, V. L. *Science* **2001**, *291*, 453.
(9) Meyer, U.; Larsson, A.; Hentze, H. P.; Caruso, R. A. *Adv. Mater.* **2002**, *14*, 1768.
(10) Jeong, U. Y.; Ryu, D. Y.; Kim, J. K.; Kim, D. H.; Russell, T. P.; Hawker, C. J. *Adv. Mater.* **2003**, *15*, 1247.
(11) Zhang, G.; Fu, N.; Zhang, H.; Wang, J.; Hou, X.; Yang, B.; Shen, J.; Li, Y.; Jiang, L. *Langmuir* **2003**, *19*, 2434.
(12) Kim, J. Y.; Yoon, S. B.; Kooli, F.; Yu, J. S. *J. Mater. Chem.* **2001**, *11*, 2912.
(13) Yilmaz, E.; Ramström, O.; Möller, P.; Sanchez, D.; Mosbach, K. *J. Mater. Chem.* **2002**, *12*, 1577.
(14) Johnson, S. A.; Ollivier, P. J.; Mallouk, T. E. *Science* **1999**, *283*, 963.
(15) Cassagneau, T.; Caruso, F. *Adv. Mater.* **2002**, *14*, 34.
(16) Wang, Y. J.; Yu, A. M.; Caruso, F. *Angew. Chem., Int. Ed.* **2005**, *44*, 2888.
(17) Zalusky, A. S.; Olayo-Valles, R.; Taylor, C. J.; Hillmyer, M. A. *J. Am. Chem. Soc.* **2001**, *123*, 1519.
(18) Urbas, A. M.; Maldovan, M.; DeRege, P.; Thomas, E. L. *Adv. Mater.* **2002**, *14*, 1850.
(19) Jang, J.; Bae, J. *Chem. Commun.* **2005**, 1200.
(20) Krause, B.; Diekmann, K.; van der Vegt, N. F. A.; Wessling, M. *Macromolecules* **2002**, *35*, 1738.
(21) Mendelsohn, J. D.; Barrett, C. J.; Chan, V. V.; Pal, A. J.; Mayes, A. M.; Rubner, M. F. *Langmuir* **2000**, *16*, 5017.
(22) Hiller, J.; Mendelsohn, J. D.; Rubner, M. F. *Nat. Mater.* **2002**, *1*, 59.
(23) Fery, A.; Schöler, B.; Cassagneau, T.; Caruso, F. *Langmuir* **2001**, *17*, 3779.

10.1021/cm061626c CCC: $33.50
Published on Web 10/21/2006

Scheme 1. Scheme for Fabricating Porous Polymer Films from [(SiO_2 NP/PAA)/PAH] Multilayers

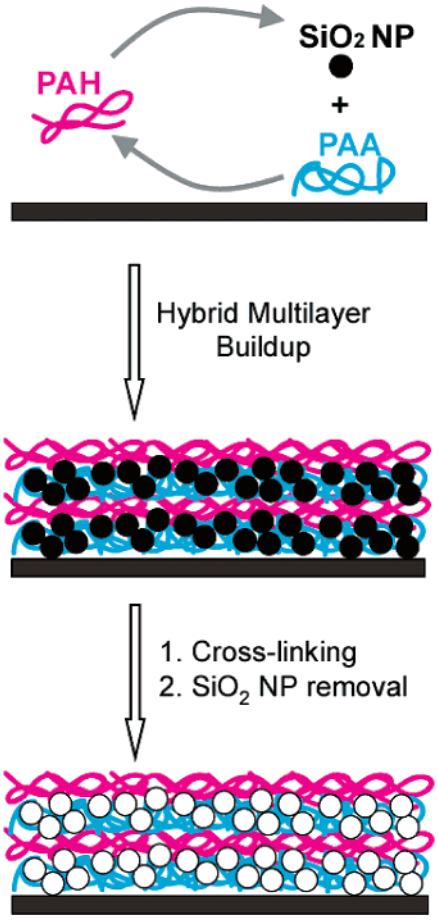

A multilayer thin film is formed by adsorbing a blend of SiO_2 NPs and PAA in alternation with PAH on a PEI-modified substrate. The film is then cross-linked, forming amide linkages between PAA and PAH, followed by the removal of SiO_2 NPs with HF/NH_4F to make the porous structure.

controlled.[24−27] Using this approach, we recently reported a polyelectrolyte templating approach for introducing porosity in PEM thin films.[28] In that work, a blend of polyelectrolyte (PAH) and hydrogen-bonding polymer (poly(4-vinylpyridine), P4VP) was assembled in alternation with PAA to construct a composite multilayer thin film as a precursor. Nanoporous thin films were then prepared by chemically cross-linking the electrostatic components (PAA/PAH) and removing the hydrogen-bonding polymer (P4VP) by increasing the pH. This approach is significant because it can be adapted to various PEM systems where two components are fixed and a third can be removed.

Building on our previous work where multilayer thin films were fabricated from three flexible polyelectrolytes, herein, we demonstrate the fabrication of nanoparticle/polyelectrolyte hybrid multilayers assembled from PAH in alternation with a blend of silica nanoparticles (SiO_2 NPs) and PAA. SiO_2 NPs are well-suited as templates to make porous films with well-defined size and shape, as they are charged and stable and can be easily removed. In this work, the nanoparticle/polyelectrolyte composite films were used as precursors for nanoporous polymer films with controlled pore size (Scheme 1). This was achieved by chemical cross-linking of the PAA/PAH and removal of the SiO_2 NPs by dissolution with ammonium fluoride-buffered hydrofluoric acid (HF/NH_4F). The method is suitable for creating LbL thin films with controlled nanostructure. Furthermore, we report the adsorption of tunable quantities of protein in the porous thin films, which makes them attractive candidates for biosensing and biocatalysis applications.

Experimental Section

Materials. PAA (M_w = 30000 g mol^{-1}), PAH (M_w = 70000 g mol^{-1}), poly(sodium 4-styrenesulfonate) (PSS, M_w = 70000), poly(ethyleneimine) (PEI, M_w = 25000 g mol^{-1}), 2-morpholinoethane sulfonic acid (MES), 1-ethyl-3-(3-dimethylaminopropyl) carbodiimide (EDC), and bovine serum albumin (BSA) were obtained from Sigma-Aldrich. SiO_2 colloidal suspensions in water were purchased from Nissan Chemical Industries, Ltd. The diameters of the SiO_2 NPs were 25 ± 5 nm (ST-50, 671 mg mL^{-1}), 45 ± 5 nm (ST-20L, 235 mg mL^{-1}), and 85 ± 15 nm (ST-ZL, 536 mg mL^{-1}), as determined from transmission electron microscopy (TEM). All materials were used as received without further purification. High-purity water was obtained from a Millipore RiOs/MilliQ system and had a resistivity greater that 18 MΩ-cm. Quartz crystal microbalance (QCM) electrodes (resonant frequency = 9 MHz, AT-cut) were purchased from Kyushu Dentsu (Nagasaki, Japan) and silicon wafers from MMRC Pty Ltd., Australia. The RCA protocol (sonication in a 1:1 mixture of water and 2-propanol for 15 min, followed by heating at 70 °C for 10 min in a 5:1:1 mixture of water, H_2O_2 (30 wt % in water), and a 29 wt % ammonia solution) was applied to clean the silicon wafers and hydrophilize the wafer surfaces. QCM electrodes were cleaned by treatment with a sulfuric acid/hydrogen peroxide (3:1) mixture (Piranha solution). (***Caution!*** *Piranha solution is highly corrosive. Extreme care should be taken when handling Piranha solution and only small quantities should be prepared.*) The nanoparticle/polyelectrolyte blend dispersions were prepared to contain 10 mg mL^{-1} SiO_2 NPs and 1 mg mL^{-1} PAA, in 0.1 M sodium chloride (NaCl). All other polymer solutions were prepared to a concentration of 1 mg mL^{-1} with 0.1 M NaCl. The pH of the dispersions/solutions was adjusted using hydrochloric acid (HCl) or sodium hydroxide (NaOH). The pH of each dispersion/solution was measured with a Mettler-Toledo MP220 pH meter.

Preparation of Nanoparticle/Polymer Hybrid Multilayer Films. Substrates were first exposed to a solution of PEI (1 mg mL^{-1}, 0.1 M NaCl) for 15 min and then rinsed by three sequential dips into Milli-Q water (1 min each), followed by drying with a gentle stream of nitrogen. For silicon wafers, the substrates were then dipped into an anionic blend dispersion of SiO_2 NPs (10 mg mL^{-1}) and PAA (1 mg mL^{-1}) at pH 9 for 15 min, followed by the same rinsing and drying protocol as described above. Multilayer films were then assembled by continuing this sequential adsorption process, alternating between cationic polyelectrolyte (PAH, 1 mg mL^{-1}, pH 5 or pH 9) and the anionic dispersions (SiO_2 NP/PAA blends) until the desired layer number was reached. For QCM electrodes, after the PEI layer, the substrates were first dipped into PSS and then PAH to obtain a bilayer (PSS/PAH) precursor to provide a uniformly charged surface. Thereafter, the film was exposed to the SiO_2 NP−PAA blend dispersion in alternation with PAH using the same protocol as above.

(24) Cho, J.; Quinn, J. F.; Caruso, F. *J. Am. Chem. Soc.* **2004**, *126*, 2270.
(25) Quinn, J. F.; Yeo, J. C. C.; Caruso, F. *Macromolecules* **2004**, *37*, 6537.
(26) Sui, Z. J.; Schlenoff, J. B. *Langmuir* **2003**, *19*, 7829.
(27) Debreczeny, M.; Ball, V.; Boulmedais, F.; Szalontai, B.; Voegel, J. C.; Schaaf, P. *J. Phys. Chem. B* **2003**, *107*, 12734.
(28) Li, Q.; Quinn, J. F.; Caruso, F. *Adv. Mater.* **2005**, *17*, 2058.

Quartz Crystal Microgravimetry (QCM). A QCM device with a frequency counter was used to determine the mass deposited after each adsorption step, according to the Sauerbrey equation.[29] The resonant frequency of the gold-coated electrodes (area 1.59×10^{-5} m^2) was ca. 9 MHz. The connections of the QCM were sealed and protected with silicone rubber gel to prevent degradation during immersion in the solutions.

Cross-linking of Multilayer Films. Cross-linking of the multilayers was performed by immersion of the multilayer-coated substrates into a solution of EDC (50 mg mL^{-1}) in MES aqueous buffer (0.05 M, pH 5.5) for 2 h to form amide bonds. After the reaction, the multilayers were washed three times with Milli-Q water.

Removal of SiO_2 Templates. The solution used for dissolving SiO_2 templates was a mixture of 2 M HF and 8 M NH_4F at pH $\sim$ 5.[30] Up to 5 min was allowed for dissolution of the silica NPs.

Atomic Force Microscopy (AFM). AFM images of air-dried multilayer films on silicon wafers were taken with a Nanoscope IIIa multimode microscope (Digital Instruments Inc., Santa Barbara, CA) operated in tapping mode.

Transmission Electron Microscopy (TEM). TEM measurements were performed on a Philips CM120 BioTWIN microscope operated at 120 kV. Samples for TEM were prepared by direct LbL deposition of multilayers upon Formvar-coated copper grids (PEI as the precursor layer) followed by EDC cross-linking and HF/NH_4F treatment.

Protein Adsorption. Thin films on QCM electrodes were dipped into BSA solution (0.5 mg mL^{-1} in 50 mM phosphate buffer at pH 7) overnight for protein adsorption, followed by rinsing with Milli-Q water and then drying under N_2.

Results and Discussion

Colloidal SiO_2 NPs with different sizes and PAA were premixed to make blend solutions at pH 9. The blend solutions used for LbL assembly contained 10 mg mL^{-1} SiO_2 NPs and 1 mg mL^{-1} PAA. Dynamic light scattering (DLS) was used to compare the particle size of SiO_2 NPs before and after mixing with PAA and indicated that there was less than 5% change in particle size. This indicates that there was no significant aggregation caused by mixing with PAA.

The formation of multilayers from a blend of SiO_2 NPs and PAA adsorbed alternately with PAH was followed by QCM. A precursor trilayer of PEI/PSS/PAH was adsorbed onto the QCM electrodes before the nanoparticle−polyelectrolyte multilayer assembly. To examine the effect of pH and particle size on LbL assembly, SiO_2 NP/PAA blends with different particle sizes were assembled with PAH at pH 5 (fully charged, $pK_a \sim 8.5$[31]) or at pH 9 (partly uncharged). Figure 1a shows the film buildup of (SiO_2 NP/PAA)/PAH at pH 5 and Figure 1b at pH 9. The QCM frequency change, $-\Delta F$, which is proportional to the mass adsorbed, was used to follow the film buildup. QCM measurements were performed in air to ensure that the films were sufficiently rigid as to allow correlation of mass with the frequency change, via the Sauerbrey relationship. Notley and co-workers have shown that QCM results of PAA/PAH multilayers obtained in water also obey this relationship.[32]

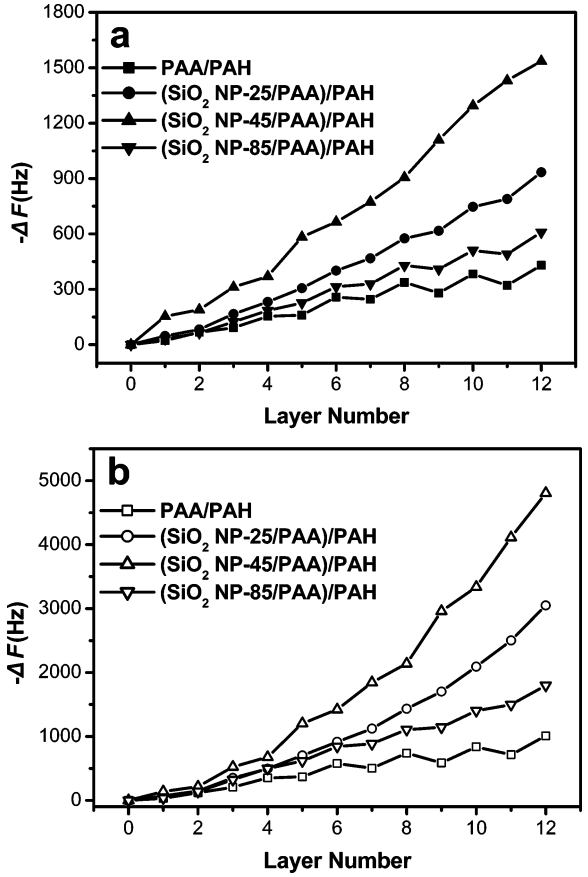

Figure 1. QCM frequency changes as a function of layer number for (SiO_2 NP/PAA)/PAH multilayer films assembled from SiO_2 NP/PAA blend solutions at pH 9 and PAH at pH 5 (a) or pH 9 (b). The SiO_2 NP size in the blend adsorption solutions was varied between 25, 45, and 85 nm.

Nevertheless, we note that the adsorbed particles do not constitute an entirely uniform film (see later), which should be taken into account when interpreting the data. Figure 1 indicates that multilayer film growth occurs when SiO_2 NP/PAA blends are alternately adsorbed with PAH at both PAH solution conditions of pH 5 and 9. The films formed from the SiO_2 NP blend with SiO_2 NP-45 (diameter 40−50 nm) grow more substantially by mass with PAH than those assembled from SiO_2 NP-25 (diameter 20−30 nm) or SiO_2 NP-85 (diameter 70−100 nm). That is, at the same SiO_2 NP wt %, the SiO_2 NP-45 yield the largest film adsorption, followed by those formed from SiO_2 NP-25 and SiO_2 NP-85. These results can be explained in terms of both particle mass and surface coverage. While the size of the SiO_2 NPs (and therefore the mass of the individual particles) increased, the surface coverage of SiO_2 NPs (which is dependent on the interaction between SiO_2 NPs and the surface, and the nanoparticle concentration in the blend adsorption solutions) decreased. The results show that film growth is maximal for 45 nm silica nanoparticles and then decreases when using 85 nm silica nanoparticles. This is due to the surface coverage of the 85 nm particles on the film being much less than that of the 25 and 45 nm particles in the blend system (see later). This is in contrast to the result reported by Kunitake and co-workers in multilayer films prepared from poly(dial-

(29) Sauerbrey, G. *Z. Phys.* **1959**, *155*, 206.
(30) Shimizu, K.; Cha, J.; Stucky, G. D.; Morse, D. E. *Proc. Natl. Acad. Sci. U.S.A.* **1998**, *95*, 6234.
(31) Choi, J.; Rubner, M. F. *Macromolecules* **2005**, *38*, 116.
(32) Notley, S. M.; Eriksson, M.; Wågberg, L. *J. Colloid Interface Sci.* **2005**, *292*, 29.

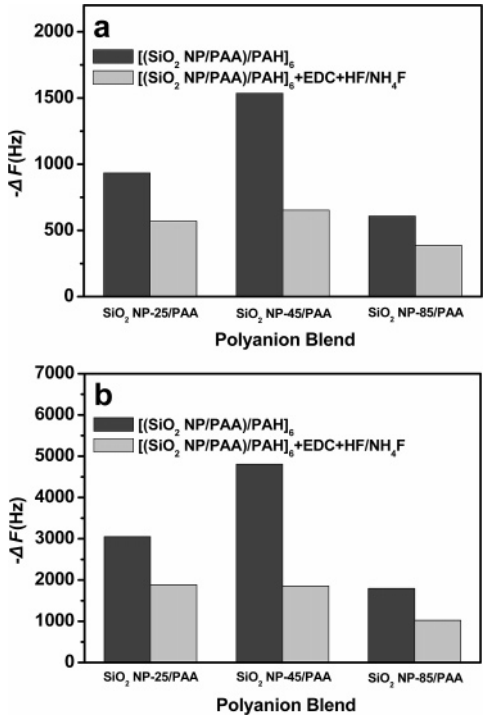

Figure 2. Total QCM frequency change for the $[(SiO_2\ NP/PAA)/PAH]_6$ multilayer films assembled from SiO_2 NP/PAA blend solutions at pH 9 and PAH at pH 5 (a) or pH 9 (b). Films before (dark) and after (gray) EDC cross-linking and exposure to HF/NH_4F to remove the SiO_2 NPs were analyzed. The error in the frequency data is ±10%.

lyldimethylammonium chloride)/SiO_2 NPs.[33] As a control, LbL film assembly between PAA at pH 9 and PAH at pH 5 or pH 9 was also investigated by QCM. It was found that these films contain less mass than any of the films prepared from the SiO_2 NP/PAA blends and PAH. Moreover, film buildup (in terms of mass) using PAH at pH 9 is about 3 times larger than that obtained using PAH at pH 5 for all the (SiO_2 NP/PAA)/PAH multilayers, and for the control multilayer PAA/PAH. This is attributed to the PAH being less charged at pH 9 and being adsorbed on the substrates with a more coiled conformation. At pH 5, PAH is highly charged, which leads to its adsorption with a less coiled conformation.

The silica NPs within the nanoparticle/polyelectrolyte hybrid multilayer films were removed by dissolution with HF/NH_4F at pH ∼ 5.[30] These conditions have been previously used to dissolve silica spheres.[35] Figures 2a and 2b show the QCM frequency changes of ((SiO_2 NP/PAA)/PAH (pH 5))$_6$ and ((SiO_2 NP/PAA)/PAH (pH 9))$_6$ films before and after exposure to HF/NH_4F, respectively. The multilayer films were exposed to HF/NH_4F until the QCM frequency reached a steady value, and the difference between before and after HF/NH_4F exposure was taken to correspond to the amount of silica within the multilayer films. It was found that the silica amount was largest for the (SiO_2 NP-45/PAA)/PAH films: 57 wt % for PAH assembled at pH 5 and 61 wt % for PAH assembled at pH 9. This is considerably more

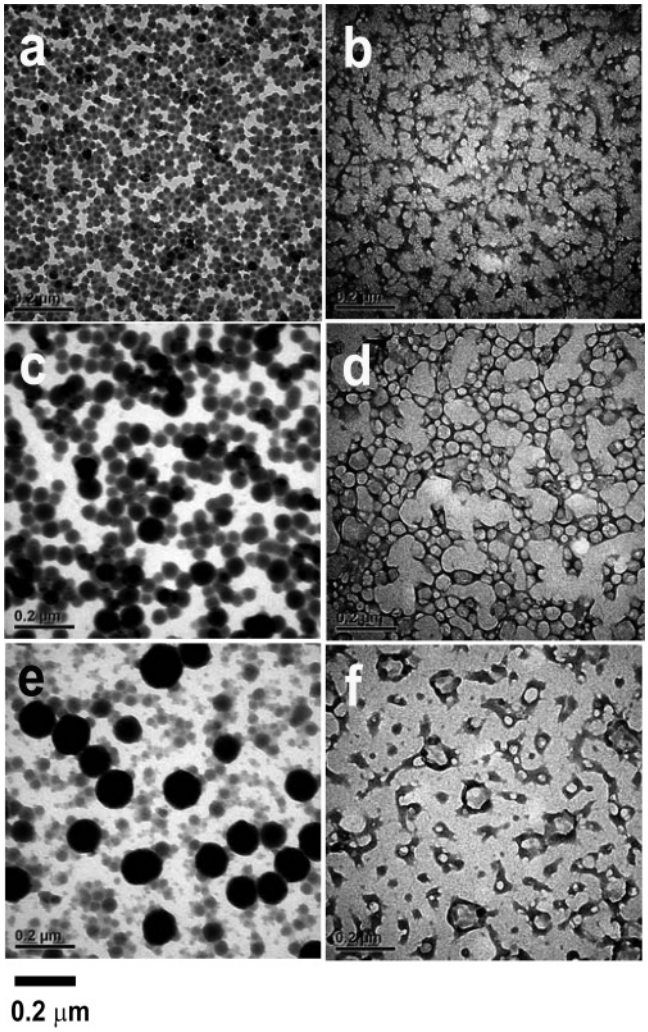

Figure 3. TEM images of the $[(SiO_2\ NP/PAA)/PAH]_4$ multilayer films assembled from PAH (at pH 5) and SiO_2 NP/PAA blend solutions (at pH 9) with different SiO_2 NP size: (a, b) SiO_2 NP-25, (c, d) SiO_2 NP-45, and (e, f) SiO_2 NP-85. Images a, c, and e are before and b, d, and f are after EDC cross-linking and exposure to HF/NH_4F to remove the SiO_2 NPs. The scale bar corresponds to all the images (a−f).

than that in either (SiO_2 NP-25/PAA)/PAH (39% for pH 5, 38% for pH 9) or (SiO_2 NP-85/PAA)/PAH (37% for pH 5, 43% for pH 9) films. Assuming the pores retain their structure after SiO_2 dissolution (which is not applicable for the films assembled with PAH at pH 9, see TEM results below), the pore volume within the porous films can be estimated from the mass lost from the QCM data. The results obtained are 1.7×10^{-13}, 4.3×10^{-13}, and 1.1×10^{-13} m^3, respectively, for the SiO_2 NP-25, SiO_2 NP-45, and SiO_2 NP-85 derived films, showing that the film prepared from SiO_2 NP-45 induced the highest pore volume. As a control (i.e., without added SiO_2 NPs in the anionic solution), the polyelectrolyte multilayers $(PAA/PAH)_6$ showed negligible frequency changes after EDC cross-linking and exposure to HF/NH_4F (pH ∼ 5). Further, when nanoparticle multilayers (SiO_2 NP-25/PAH)$_6$ were prepared without blending, almost the entire film (97 wt %) disassembled after HF/NH_4F treatment. This indicates that the third component (PAA) is necessary to stabilize the porous films.

The nanoparticle−polyelectrolyte hybrid multilayer films ((SiO_2 NP/PAA)/PAH (pH 5))$_4$ were characterized by TEM both before and after silica removal. Figures 3a, 3c, and 3e

(33) Lvov, Y.; Ariga, K.; Onda, M.; Ichinose, I.; Kunitake, T. *Langmuir* **1997**, *13*, 6195.
(34) Itano, K.; Choi, J.; Rubner, M. F. *Macromolecules* **2005**, *38*, 3450.
(35) Yu, A. M.; Wang, Y. J.; Barlow, E.; Caruso, F. *Adv. Mater.* **2005**, *17*, 1737.

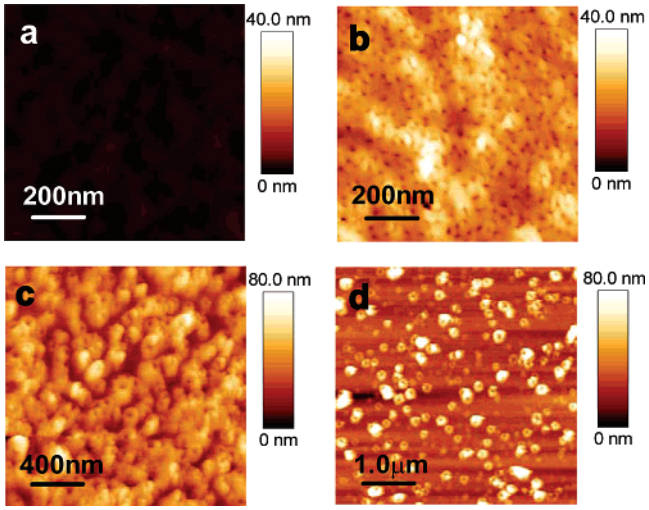

Figure 4. AFM images of the $[(SiO_2$ NP/PAA)/PAH$]_6$ multilayer films assembled from PAH (at pH 5) and SiO_2 NP/PAA blend solutions (at pH 9): (a) no SiO_2 NP, (b) SiO_2 NP-25 (25 ± 5 nm), (c) SiO_2 NP-45 (45 ± 5 nm), and (d) SiO_2 NP-85 (85 ± 15 nm). Images were collected after EDC cross-linking and exposure to HF/NH_4F to remove the SiO_2 NPs.

show TEM images of films before HF/NH_4F (pH 5) exposure, which indicate that the particle sizes of SiO_2 NPs within the multilayers $((SiO_2$ NP-25/PAA)/PAH$)_4$, $((SiO_2$ NP-45/PAA)/PAH$)_4$, and $((SiO_2$ NP-85/PAA)/PAH$)_4$ were 25 ± 5, 45 ± 5, and 85 ± 15 nm, respectively. TEM images also showed that the number of SiO_2 NPs in the films decreased as the nanoparticle size increased. After HF/NH_4F exposure, the resulting pores (bright area with surrounding darker area) were randomly distributed over the films (Figures 3b, 3d, and 3f)). The pore sizes of the films induced by SiO_2 NP removal (as determined from the TEM images) closely correspond to the sizes of the SiO_2 NPs used during multilayer assembly. The irregular bright domains also evident in the TEM images are due to the deposition of PAA/PAH multilayer film between the adsorbed SiO_2 NPs. These areas are also observed in the TEM images before silica removal. The TEM results demonstrate that the pore size could be controlled by using different sizes of SiO_2 NPs for assembly. The multilayer films $((SiO_2$ NP/PAA)/PAH (pH 9$))_4$ before and after silica removal were also characterized by TEM. In this case, a porous structure could not be observed under TEM. This may be attributed to a larger number of SiO_2 NPs adsorbing during the LbL buildup of $((SiO_2$ NP/PAA)/PAH (pH 9$))_4$ (Figure 1). Therefore, the SiO_2 NPs induced pores that merged together (and not discrete, individual pores) during HF exposure.

The porous multilayer films (PAH assembled at pH 5) were further characterized by AFM to probe the surface morphology of the films. Figures 4b−d show the surface images of the multilayer films $((SiO_2$ NP-25/PAA)/PAH$)_6$, $((SiO_2$ NP-45/PAA)/PAH$)_6$, and $((SiO_2$ NP-85/PAA)/PAH$)_6$ after silica nanoparticle removal. Pore sizes were estimated by examining the height profile in the vicinity of the pores and were determined to be 25 ± 5, 45 ± 5, and 85 ± 15 nm for the $((SiO_2$ NP-25/PAA)/PAH$)_6$, $((SiO_2$ NP-45/PAA)/PAH$)_6$, and $((SiO_2$ NP-85/PAA)/PAH$)_6$ films, respectively. Again, it is clear from the AFM images that the number of pores in the films decreased as the size of the nanoparticles increased, which further confirms the TEM results. As a control, a (PAA/PAH$)_6$ film was EDC cross-linked and exposed to HF/NH_4F (pH $\sim$ 5) and then imaged by AFM. Figure 4a indicates that no porous structure was observed and that the film surface was very smooth (surface roughness $\sim$ 0.5 nm). This suggests that the porous structure of the $((SiO_2$ NP/PAA)/PAH$)_6$ films after HF exposure is not due to film rearrangement but is the result of replication of SiO_2 NP templates. As with TEM analysis, $((SiO_2$ NP/PAA)/PAH (pH 9$))_6$ multilayer films did not show any evidence of SiO_2 NP-induced porosity following removal of the SiO_2 NPs.

To determine whether or not the porous structure extends throughout the entire film, 4-, 6-, and 8-bilayer films of $(SiO_2$ NP-25/PAA)/PAH (pH 5) were characterized by TEM after silica NP removal. These films were formed directly on TEM grids with PEI as the precursor layer. Unlike AFM, which reveals surface morphology, TEM permits observation throughout the films. From Figures 5a−c, it is evident that the pore number and total pore volume within the films increases as the bilayer number of the assembled multilayer films increases, which is in accordance with the QCM results on film buildup (Figure 2). The TEM results demonstrate that the porous structure induced in $(SiO_2$ NP-25/PAA)/PAH (pH 5) after EDC cross-linking and HF/NH_4F exposure not only is on the film surface but also extends throughout the film.

To investigate the interaction between proteins and the multilayer films, BSA (isoelectric point 4.5, $M_w = 67$ KDa) was adsorbed overnight at pH 7 in PBS buffer onto the $((SiO_2$ NP/PAA)/PAH$)_n$ films both before and after SiO_2 NP removal. QCM was used to determine the adsorbed amount

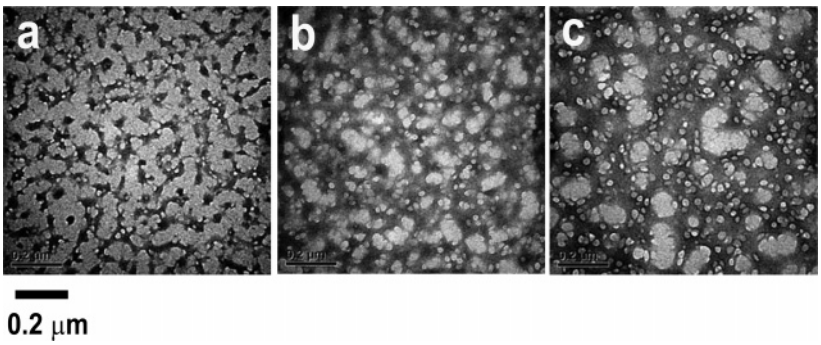

Figure 5. TEM images of the $[(SiO_2$ NP-25/PAA)/PAH$]_n$ multilayer films with bilayer number $n = 4$ (a), 6 (b), and 8 (c) deposited from PAH (at pH 5) and SiO_2 NP-25/PAA blend solutions (at pH 9). Images were collected after EDC cross-linking and exposure to HF/NH_4F to remove the SiO_2 NPs. The scale bar corresponds to all the images (a−c).

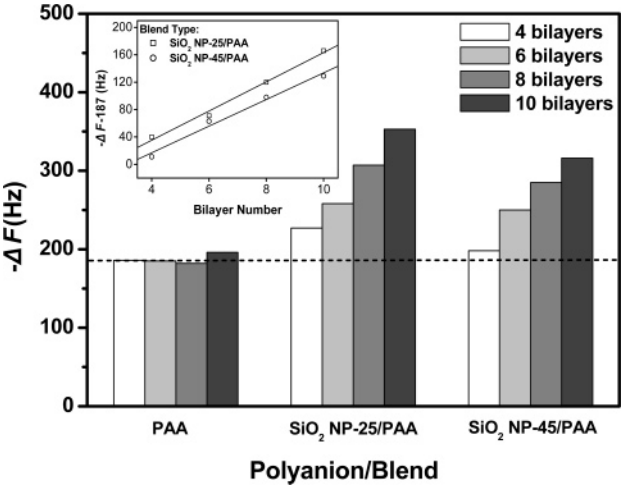

Figure 6. Net QCM frequency changes as a function of film bilayer number for the adsorption of BSA on the films constructed by the alternate deposition of (SiO_2 NP/PAA)/PAH (pH = 5) followed by EDC cross-linking and exposure to HF/NH_4F. The inset graph is the relationship between net BSA adsorption within the films ($-\Delta F$)−187 and film bilayer number.

of protein on the multilayer films composed of (SiO_2 NP-25/PAA)/PAH (pH 5) and (SiO_2 NP-45/PAA)/PAH (pH 5). For each film type, films of 4-, 6-, 8-, and 10-bilayer were examined. The frequency change after BSA was adsorbed onto the porous films increased systematically with increasing bilayer number (Figure 6), suggesting that BSA infiltrates into the porous films. The larger amount of BSA adsorbed onto the films derived from 25 nm SiO_2 particles, than on the films prepared from 45 nm SiO_2 particles, is likely to be due to a combination of the larger number of pores in the films prepared from the SiO_2 NP-25 and differences in the final pore structure of the films. To understand whether the protein adsorption was confined to the film surface, the adsorption onto PAA/PAH (pH 5) multilayers with different bilayer numbers was also investigated. A constant BSA adsorption amount (∼187 Hz frequency change) was observed for all bilayer numbers studied (Figure 6), which suggested protein permeation into the PAA/PAH films was minimal, and therefore the protein was mainly adsorbed on the film surface. The BSA adsorption within the porous films less the amount expected on the film surface, $-\Delta F$ −187 (Figure 6, inset), indicates that the BSA adsorbed amount within the films increases linearly with increasing bilayer number. As a further control, BSA adsorption onto the ((SiO_2 NP/PAA)/PAH)$_n$ films with 4-, 6-, 8-, and 10-bilayers *before HF etching* was also investigated. The results (data not shown) reveal that the frequency change due to BSA adsorption increased slightly from 4- to 6-bilayer films and then remained almost constant ($-\Delta F \sim 230$ Hz) as the bilayer number increased further. This indicates that almost no infiltration occurs into the ((SiO_2 NP/PAA)/PAH)$_n$ films and that the majority of the protein was adsorbed on the film surface. Therefore, it can be concluded that, after silica particle removal from the ((SiO_2 NP/PAA)/PAH)$_n$ multilayers, porosity extends into the films and the film permeability to proteins increases. Tuning the protein adsorption amount may make these films useful candidates for biosensing and biocatalysis applications.

Conclusions

We have demonstrated that nanoparticle−polyelectrolyte hybrid multilayers ((SiO_2 NP/PAA)/PAH) can be assembled by the alternate adsorption from a blend of colloidal silica particles and PAA, with PAH. After EDC cross-linking the PAA/PAH (forming amide linkages within the films) and dissolving the SiO_2 NPs, porous polymer films were prepared. Significantly, the pore size of the films could be controlled by using SiO_2 NP templates with different sizes in the multilayer assembly. The permeability of the films after silica particle removal increased, as demonstrated by an increased amount of BSA adsorbed with increasing bilayer number. Considering the variety of materials that could be assembled to form blended nanoparticle−polyelectrolyte films, this method provides a general approach for fabricating polymer thin films with controlled pore sizes. This approach is also likely to find application in introducing well-defined porosity in PEM capsules that are of interest in drug delivery.

Acknowledgment. The authors acknowledge funding from Australian Research Council under the Discovery Project and Federation Fellowship schemes, and from the Victorian State Government under the STI initiative. The Particulate Fluids Processing Centre at The University of Melbourne is acknowledged for providing infrastructure support.

CM061626C